6th European Conference on Computational Mechanics (ECCM 6)
7th European Conference on Computational Fluid Dynamics (ECFD 7)
1115 June 2018, Glasgow, UK

NUMERICAL STUDY OF FLOWS AROUND A SHIP HULL INCLUDING ELASTIC DEFORMATION EFFECT USING A MODE FUNCTION

KUNIHIDE OHASHI[1]

[1] National Maritime Research Institute
6-38-1 Shinkawa Mitaka Tokyo Japan
k-ohashi@nmri.go.jp

Key words: Elastic Deformation, Mode Function, Overset-Grid Method

Abstract. A numerical method to simulate the flows with the elastic deformation effects using the mode function has been developed. An in-house structured CFD solver which capable the overset-grid method is used. The elastic deformation is obtained by solving the equations based on the Bernulli-Euler beam theory, and the deformations of the 2nd and the 3rd modes are accounted for by the grid deformation method with the strong coupling way. Present method is applied to the computation of the flows around a container ship in the severe wave condition. The amplitude of the ship motions consistent with the measured data. Present method reproduce the impact pressure due to the interaction between the ship motions and incoming waves. Additionally, the effect of the elastic deformations is also examined.

1 INTRODUCTION

Recently, Reynolds Averaged Navier-Stokes(RANS) simulations are utilized at the design stage of ship performance, and the numerical simulations are gradually applied to the more complex problems. Unsteady RANS(URANS) solver which can cope with the overset-grid method is coupled with the mode function method to compute the elastic deformation of a ship hull. The elastic deformation of the ship hull is accounted by for the grid deformation and the strong coupling way. The present method is applied to the computation of the flows around a container ship hull with the incoming regular head-sea waves. The computational results of the time history of the pressure on the hull surface and the amplitude of the ship motions are compared with the measured results. Additionally, the detailed analysis of the effect of the elastic deformation is performed.

2 COMPUTATIONAL METHOD

2.1 Base solver

An in-house structured CFD solver[1] is employed. The governing equation is 3D RANS equation for incompressible flows. An artificial compressibility approach is used

for the velocity-pressure coupling. The spatial discretization is based on the finite-volume method. A cell centered layout is adopted that the flow variables are defined at the centroid of each cell and the control volume is a cell itself. The inviscid fluxes are evaluated by the third-order upwind scheme based on the flux-difference splitting of Roe. The evaluation of viscous fluxes is the second-order accurate. For unsteady flow simulations, the dual time stepping approach is used in order to recover incompressibility at each time step. It is consisted by the second order two-step backward scheme for the physical time stepping and the first order Euler implicit scheme for the pseudo time. The linear equation system is solved by the symmetric Gauss-Seidel (SGS) method.

For the free surface treatment, an interface capturing method with a single phase level set approach is employed.

Incoming Regular headsea waves are generated at the region inside of the computational domain[2]. Body motions are obtained by solving the equations of motion, and motions are accounted for by the moving grid technique with the grid deforming methodology. Grid velocities are contained in the inviscid terms to satisfy the geometrical conservation law. The grid velocities are derived from the volume where an each cell face sweeps. The boundary condition on a body is given as the velocities of the body motion.

The regions where the overset relations are composed deform with the body motions to maintain the overset information, and the amount of deformations gradually decreases with the distance from the body surfaces. Such method is adapted to avoid the computational load by using the dynamic overset-grid method.

2.2 Overset-grid method

The weight values for the overset grids interpolation are determined by an in-house system ([3]). Details of the system can be found on [3], and the summary is described.

1. The priority of the computational grid is set.

2. Two layers of cells on a higher-priority grid and facing the outer boundary are set as receptor cells to satisfy the third-order discretization of the NS solver.

3. Hole-cutting is carried out. The cells of a higher priority grid and those inside a body are identified. (called the in-wall cell herein) The cells of a lower priority grid and those inside a body are also identified. Additionally, two cells that neighbour the in-wall cells are also set as receptor cells to satisfy the third-order discretization of the NS solver.

4. Receptor cells for which the flow variables must be interpolated from donor cells are defined. Cells of a lower-priority grid, which are inside the domain of a higher-priority grid, are set as the receptor cells.

5. The Donor cell for the receptor cell is searched for at the local spline coordinate. Then, the weight values for the overset interpolation are determined by the Ferguson spline interpolation.

Procedures of determining the coefficient of the spline function and the searching for a donor cell are parallelized by the share memory type based on the OpenMP methodology. Flow variables of the receptor cell are updated when the boundary condition is set.

2.3 Mode function method

The elastic deformation is computed by the mode function method[4][5]. The equilibrium equation of the shear force and the moment on the small element which is defined by the division of the beam in the length direction and based on the Bernulli-Euler theory is given as follows:

$$\mu\frac{\partial^2 w}{\partial t^2}+\frac{\partial^2}{\partial x^2}\left(\eta EI\frac{\partial^3 w}{\partial x^2\partial t}\right)+\frac{\partial^2}{\partial x^2}\left(EI\frac{\partial^2 w}{\partial x^2}\right)=F_e \tag{1}$$

where w is the vertical displacement, μ and EI are the mass and the flexural rigidity per unit length, η is the structural damping coefficient, and F_e is the external force.

The vertical displacement w is assumed to be expressed by the superposition of the mode functions, then, w is defined as follows:

$$w(x,t)=\sum_n q_n(t)W_n(x) \tag{2}$$

where $W_n(x)$ is the shape function of the n-th mode, $q_n(t)$ is the time-dependant amplitude. The integral form of the equation (1) with the equation (2) and the weight function $W_n(x)$ which is the shape function of the own mode is given as follows:

$$\begin{aligned}\ddot{q}_n(t)\int\mu(x)W_n(x)W_n(x)dx &+ \dot{q}(t)\int\eta EI(x)\frac{d^2W_n(x)}{dx^2}\frac{d^2W_n(x)}{dx^2}dx\\ &+ q_n(t)\int EI(x)\frac{d^2W_n(x)}{dx^2}\frac{d^2W_n(x)}{dx^2}dx=\int F_eW_n(x)dx\end{aligned} \tag{3}$$

where the external force F_e contains the hydrodynamic forces on the ship-fixed coordinate and the dead weight. The rigid motions are obtained by solving the motion equation of the rigid motion, and the elastic deformations are computed by the equation (3).

The mode function which satisfies the free end condition in the both ends is defined as follows:

$$\begin{aligned}W_n(x)&=cos(\lambda_n x)+cosh(\lambda_n x)-c_n(sin(\lambda_n x)+sinh(\lambda_n x))\\ c_n&=\frac{cos(\lambda_n L)-cosh(\lambda_n L)}{sin(\lambda_n L)-sinh(\lambda_n L)}\end{aligned} \tag{4}$$

where $\lambda_n L$ is the eigenvalue of the mode, $\lambda_2 L$ is 4.730 for the second mode, and $\lambda_3 L$ is 7.853 for the third mode.

The accelerations are obtained by solving the equation (3). then, the velocity $\dot{q}$ is derived from the following equation:

$$\dot{q}^{n+1}=\dot{q}^n+\Delta t\,\ddot{q}^{n+1} \tag{5}$$

The velocity $\dot{q}$ and the displacement are obtained by the strong coupling method. The initial value of $\dot{q}$ is set as the value at the last time step. The initial value of the displacement is calculated by using the third-order Adams-Bashforce scheme, and the displacement is corrected by using the third-order Adams-Moulton scheme at the pseudo time steps to recover incompressibility.

3 COMPUTED RESULTS

The present method is applied to the flows around the container ship in the regular head waves[6][7]. The model ship length is 3.0m, and the Reylonds number is $R = 2.557 \times 10^6$, the Froude number is $Fn = 0.179$. The wave length ratio of incoming regular headsea waves is $\lambda/L = 0.8, 1.0, 1.25$, and the wave height ratio h_w/L is 0.035 that is the limit state condition to examine the structural strength. The motions are free to pitch and heave. The non-dimensional physical time step size is set to $\Delta t = 0.001$. The mass distribution is equals to the buoyancy curve, and the flexural rigidity is defined as the trapezoidal distribution[7]. The structural damping coefficient is set the value at the wet damping condition[7].

Table 1 shows the division number of the computational grids in each direction, and Figure 1 shows the global view of the grids. The computational grids consist of the ship hull and the background rectangular grids. IM means the ship length direction, JM is the width direction, and KM is the depth direction for the rectangular grid. For the ship hull grid, IM means the ship length direction, JM is the girth direction, and KM is the division number in the normal direction from the hull surface. The rectangular grid has the division number in the x-direction to divide the wave length $\lambda/L = 0.8$ by 50 divisions.

Table 1: Division number of computational grid

Grid	IM×JM×KM
Hull	129×85×45
Rect.	117×33×37

Fig.2 shows the time histories of the ship motions and the amplitude $q(t)$ of the modes, the incoming wave height at the midship of the ship hull on the one encounter period T_e at $\lambda/L = 1.0$. Besides that the ship motions have the same period with the encounter period T_e, the amplitudes of the elastic deformations have the natural period of the modes, and the amplitude of the second mode is larger than the amplitude of the third mode.

From Fig.3 to Fig.5 show the longitudinal distributions of the elastic deformation of the each mode and the total deformation at the time T_1, T_2, T_3 in the Figure 2. The stem of the ship hull is positioned at -0.5, and the midship is positioned at 0.0. On the time T_1 when the crest of the regular waves locates at the midship, the amplitude $q(t)$ takes the negative value, and the shape of the second mode takes the distribution that the crest locates at the midship. The amount of the third mode is relatively small, and the shape of the total deformation is similar with the shape of the second mode. And next, the time

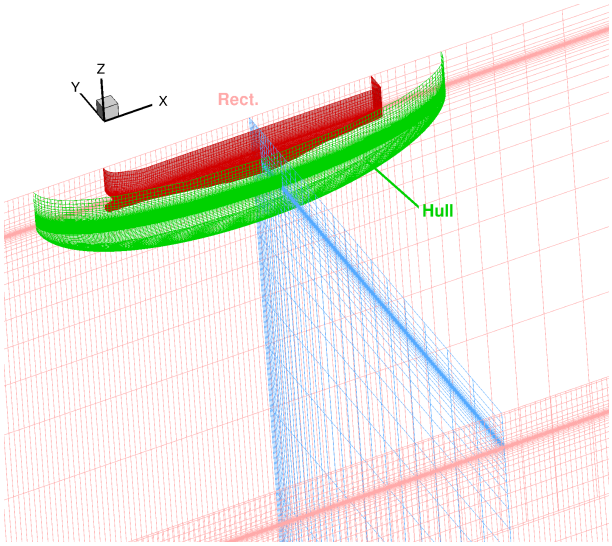

Figure 1: Computational grids

T2 that the trough of the regular waves closes to the midship, the shape of the second mode takes the distribution that the trough locates at the midship. Finally, the time T3 that the wave height is closely zero at the midship and the crest locates at the bow, the shape of the third mode is similar with the shape of the incoming wave and affects to the shape of the total deformation.

Fig.6 shows the comparisons of the wake flows near the ship stern end at the time T_2 to examine the elastic deformation effect. Although the difference of the velocity distribution near the ship hull is relatively small, the difference due to the elastic deformation can be observed in the region which is apart from the ship hull.

Fig.7 shows the comparisons of the heave and pitch motions including the elastic deformation effect. The computed results show agreement with the measured results. The effect of the elastic deformation can be found at $\lambda/L = 1.25$, and the amplitude of the motions with the elastic deformation becomes smaller than the amplitude without the elastic deformation.

Fig.8 shows the comparisons of the time history of the pressure at the position near the bow and above the still water plane, and Fig.8 shows the free surface near the bow and the measured points of the pressure at the time T_1 and T_2 in the Figure 8. On the time T_1, the points P_1 and P_2 enter to the water, and the impact pressure can be observed. Second, the time T_2, the free surface near the points P_1 and P_2 is disturbed by the interaction between the incoming regular waves and the ship motions, and the points P_1 and P_2 are close to the free surface, then, the pressure at P_1 and P_2 becomes higher value again. The present results with the elastic deformation capture the time history of the pressure, especially, the second pressure rise at P_2.

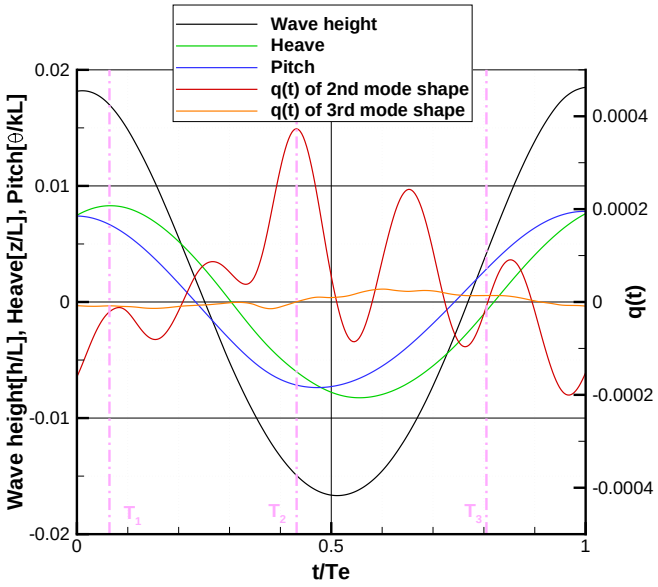

Figure 2: Time history of wave height, ship motions and q(t) of mode shapes

4 CONCLUSIONS

- The numerical method including the elastic deformation effect of the ship hull has been developed.

- The elastic deformation is obtained by solving the equations based on the Bernulli-Euler beam theory, and deformations are accounted for by the grid deformation method

- The computed results of the amplitudes of the ship motions show agreement with the measured data, and the amplitude with the elastic deformation at $\lambda/L = 1.25$ becomes smaller than the amplitude without the elastic deformation.

- The present method can trace the time history of the pressure at the points near the ship bow including the first impact pressure and capture the second rise of the pressure due to the interaction between the incoming waves and the ship motions with the elastic deformation effect.

5 ACKNOWLEDGEMENT

This work has been supported by JSPS KAKENHI Grant Number JP16K06919.

REFERENCES

[1] Ohashi, K., Hino, T., Hirata, N., Kobayashi, H., Development of NS solver with a structured overset grid method. *The 28th Computational Fluid Dynamics Symposium*. 2014

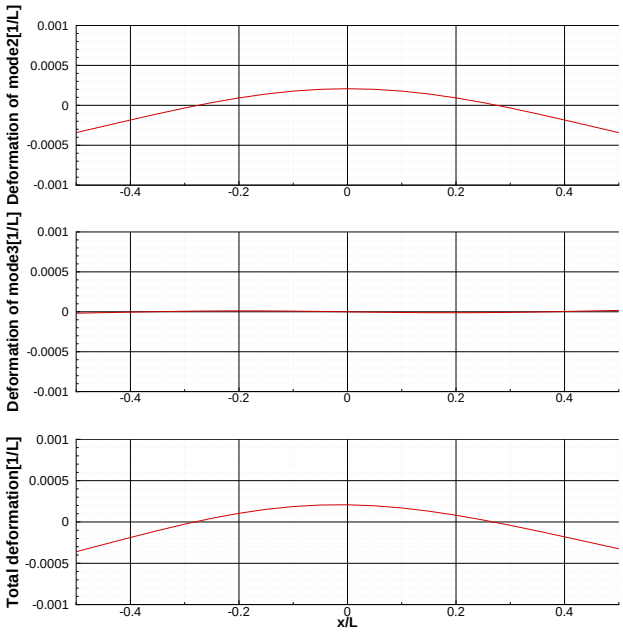

Figure 3: Elastic deformations of modes(top:2nd mode, middle:3rd mode, bottom:total) at time T_1

[2] Ohashi, K., Sakamoto, N., Hino, T., Numerical Simulation of Flows around KVLCC2 Hull Form with Ship Motions in Regular Waves, *ECCOMAS MARINE 2013*.

[3] Kobayashi, H., Kodama, Y., Developing spline based overset grid assembling approach and application to unsteady flow around a moving body, *ECCOMAS MARINE2015*.

[4] Yamamoto, Y., Fujino, M., Fukasawa, T., Motion and Longitudinal Strength of a Ship in Head Sea and the Effects of Non-Linearities.(2nd Report) *J. of the Soc. Naval Archit. Japan* (1978) 144:214-218.

[5] Mikami, T., Kashiwagi, M., Time-domain strip method with memory-effect function considering the body nonlinearity of ships in large waves(second report), *J. Mar. Sci. Tech.* (2009) 14:185-199.

[6] Oka, M., Hattori, K., Ogawa, Y., Reproduction of wave induced vibrations of a ship by using a new type backbone model, *Proc. of the 10th Research Presentation Meeting in National Maritime Research Institute*. 2010

[7] Takami, T. Oka, M., Iijima, K., Study on application of CFD and FEM coupling method to evaluate dynamic response of ship under severe wave condition, *Proc. of OMAE 2017*.

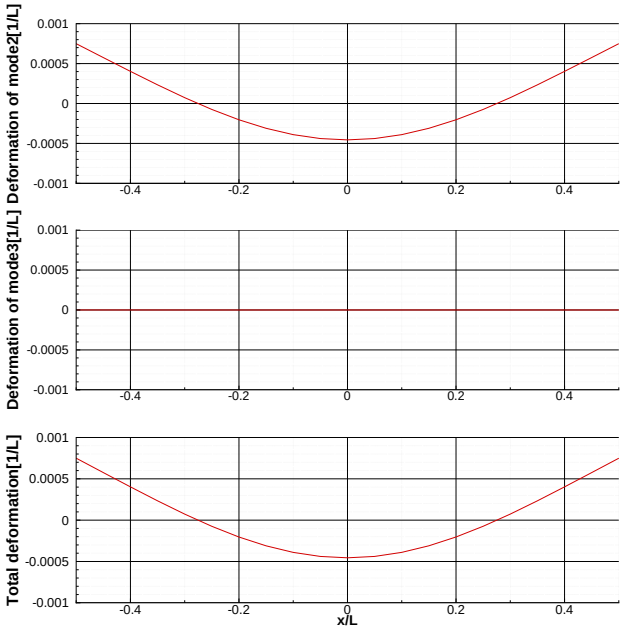

Figure 4: Elastic deformations of modes(top:2nd mode, middle:3rd mode, bottom:total) at time T_2

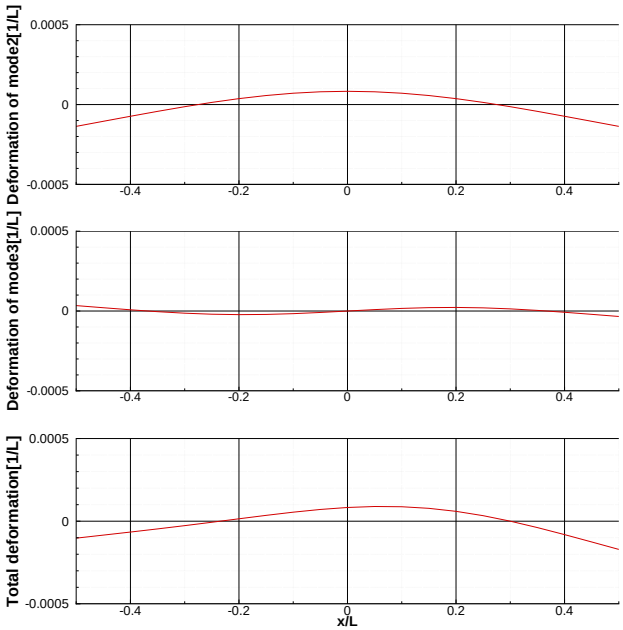

Figure 5: Elastic deformations of modes(top:2nd mode, middle:3rd mode, bottom:total) at time T_3

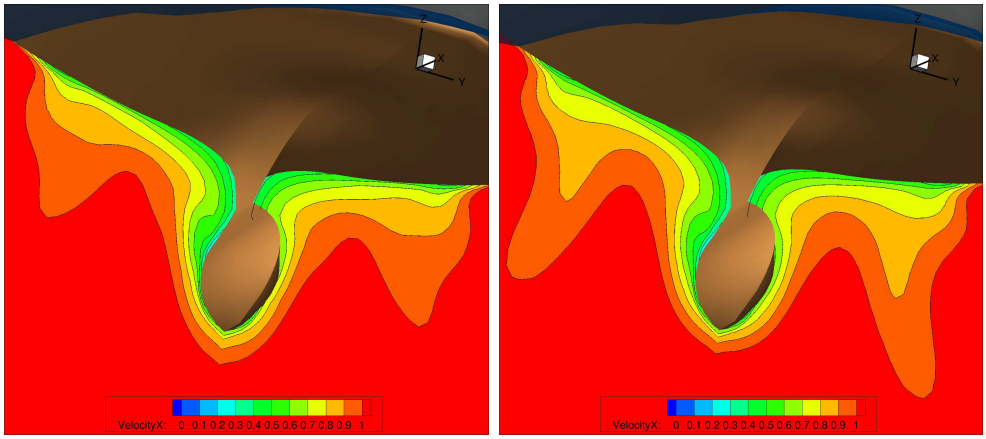

Rigid body Elastic body

Figure 6: Axial velocity contour

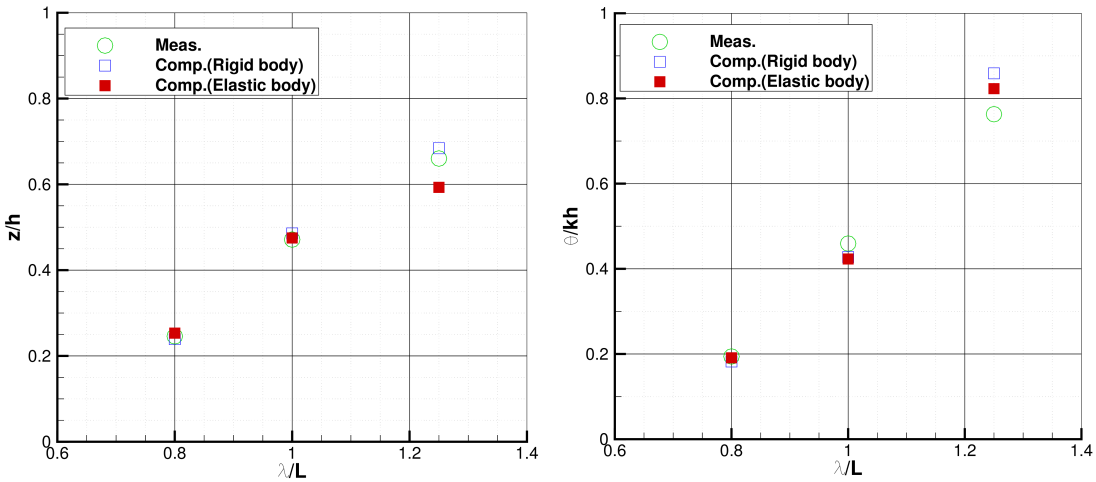

Heave Pitch

Figure 7: Comparisons of heave and pitch motion amplitudes

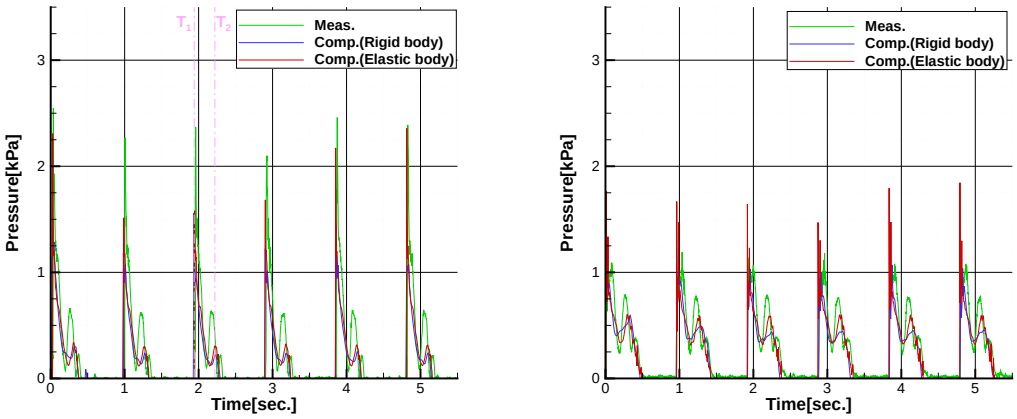

P_1 P_2

Figure 8: Comparisons of time history of pressure

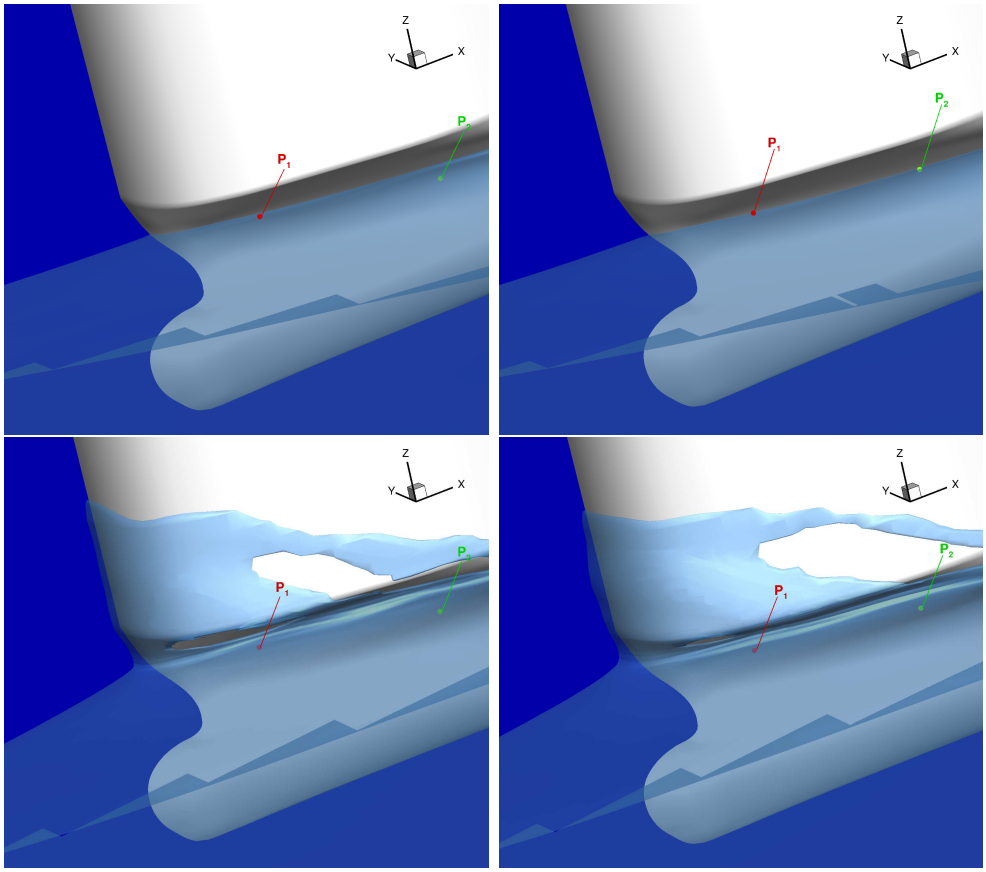

Rigid body Elastic body

Figure 9: Instantaneous view of free surface(top:T_1, bottom:T_2)